# Derivation of soil-attribute estimations from legacy soil maps

**Article** *in* Soil Research · January 2015

DOI: 10.1071/SR14274

CITATIONS
5

READS
97

**4 authors**, including:

Nathan Odgers
Landcare Research
**38** PUBLICATIONS **335** CITATIONS
SEE PROFILE

Karen W Holmes
Department of Agriculture and Food
**39** PUBLICATIONS **1,050** CITATIONS
SEE PROFILE

Craig Liddicoat
University of Adelaide
**8** PUBLICATIONS **28** CITATIONS
SEE PROFILE

**CSIRO** PUBLISHING
*Soil Research*
http://dx.doi.org/10.1071/SR14274

# Derivation of soil-attribute estimations from legacy soil maps

*Nathan P. Odgers*[A,F], *Karen W. Holmes*[B,C,D], *Ted Griffin*[B], *and Craig Liddicoat*[E]

[A]Department of Environmental Sciences, Faculty of Agriculture and Environment, C81 Biomedical Building, The University of Sydney, NSW 2006, Australia.
[B]Department of Agriculture and Food Western Australia, 3 Baron-Hay Court, South Perth, WA 6151, Australia.
[C]Soil Matrix Group, School of Earth and Environment, The University of Western Australia, Stirling Highway, Crawley, WA 6009, Australia.
[D]CSIRO Sustainable Agriculture Flagship, Ecosciences Precinct, Dutton Park 4001, Australia.
[E]Department of Environment, Water and Natural Resources, Plant Biodiversity Centre, Hackney Road, Botanic Gardens, Adelaide, SA 5001, Australia.
[F]Corresponding author. Email: nathan.odgers@sydney.edu.au

**Abstract.** It is increasingly necessary to apply quantitative techniques to legacy soil polygon maps given that legacy soil maps may be the only source of soil information over large areas. Spatial disaggregation provides a means of extracting information from legacy soil maps and enables us to downscale the original information to produce new soil class maps at finer levels of detail. This is a useful outcome in its own right; however, the disaggregated soil-class coverage can also be used to make digital maps of soil properties with associated estimates of uncertainty. In this work, we take the spatially disaggregated soil-class coverage for all of Western Australia and the agricultural region of South Australia and demonstrate its application in mapping clay content at six depth intervals in the soil profile. Estimates of uncertainty are provided in the form of the 90% prediction interval. The work can be considered an example of harmonisation to a common output specification. The validation results highlighted areas in the landscape and taxonomic spaces where more knowledge of soil properties is necessary.

**Additional keywords:** clay content, digital soil mapping, legacy soil data, prediction interval, spatial disaggregation, weighted mean.

Received 1 October 2014, accepted 31 March 2015, published online 29 July 2015

## Introduction

Soil mapping has been carried out in Australia since the mid-19th Century. Since then, effort has often focused on mapping the spatial distribution of soil or land classes and, as such, has often been associated with developments in soil classification (Gibbons 1983).

Legacy soil polygon maps depict the spatial distribution of soil map units efficiently but they do not usually depict the spatial distribution of the soil classes that compose those soil map units. This is typically a result (and limitation) of the scale of mapping, where map units cannot be delineated finely enough to distinguish between the distinct soil classes that occur across the landscape. To capture the information, map units are defined at a pre-defined mapping scale and component soils are documented in a summary fashion within associated data tables or reports. Spatial disaggregation attempts to downscale the soil map-unit information in order to map the spatial distribution of the individual soil classes. Many spatial disaggregation studies have been published in the last few years, for example Bui and Moran (2001), Sun *et al*. (2010), Thompson *et al*. (2010), Häring *et al*. (2012), Nauman and Thompson (2014), Subburayalu *et al*. (2014) and Odgers *et al*. (2014*b*).

The product of spatial disaggregation of a legacy soil polygon map is usually a raster map depicting a soil-class prediction for every grid cell; however, some spatial disaggregation algorithms have demonstrated the ability to produce maps of the estimated probabilities of occurrence for each soil class too (e.g. Odgers *et al.* 2014*b*). A benefit of these products is that we can see how the probabilities vary smoothly across the landscape; this may be a more realistic depiction of the soil variability than a hardened map showing mere presence or absence.

The question then becomes: how can we use the disaggregated maps to make maps of soil properties? With legacy soil polygon maps, it is usually a matter of calculating the within-map-unit weighted mean of the target soil property using the areal extent of the constituent soil classes as weights (e.g. Galbraith *et al.* 2003; Odgers *et al.* 2012). The weighted mean property value is spatially invariant within map unit polygons. We can apply a similar technique to disaggregated soil-class maps; the result is similar but the spatial pattern of the soil-property distribution is much more detailed (e.g. Thompson *et al.* 2010).

On the other hand, it is possible to generate soil-property maps where the values vary smoothly from grid cell to grid cell

if the spatial disaggregation yields a set of soil-class probability rasters (e.g. Odgers *et al.* 2015). Here, the weights in the weighted mean soil-property calculation are the probabilities of occurrence of the soil classes, which vary from grid cell to grid cell. The Soil Land Inference Model (SoLIM) infers soil properties by the same mechanism, although in that case the weights are soil-class memberships derived by a semi-automated expert-driven process (e.g. Zhu and Band 1994; Zhu *et al.* 2001, 1997).

Furthermore, it is becoming increasingly desirable to have knowledge of the uncertainty associated with digital soil-property predictions, which can then be used, for example, to forecast outcomes under a range of different management scenarios. The soil-class rasters can also be used to estimate this uncertainty. To do so, estimates of the within-soil-class variability in the target soil property must be known (which themselves are subject to uncertainty). Mechanisms for assessing this variability quantitatively have occasionally been built into legacy soil survey (e.g. Pásztor *et al.* 2010), but more frequently, estimates have been based on expert judgement informed by fieldwork and limited site observations (Soil Survey Staff 2006), or have been computed after the fact from limited site observations (e.g. Odgers *et al.* 2015). Often, the number of samples available for characterising the within-soil-class variability is inadequate (Arnold 1966; Protz *et al.* 1968; Taylor 1970).

### *The TERN project, spatial disaggregation and digital soil-property mapping*

The Australian Federal Government has funded the Terrestrial Ecology Research Network (TERN) since 2012. TERN's Australian Soil Grid Facility is building a new set of digital soil-property maps for Australia according to the GlobalSoilMap specifications (GlobalSoilMap Science Committee 2013). Under the specifications, digital soil-property maps will be produced for six depth intervals: 0–5, 5–15, 15–30, 30–60, 60–100 and 100–200 cm. Property estimates will be accompanied by estimates of uncertainty in the form of the 90% prediction interval (PI) limits about the predicted values (Grundy *et al.* 2015; Viscarra Rossel *et al.* 2015).

As part of the TERN effort, digital soil property maps that conform to the GlobalSoilMap standards have been produced from spatially disaggregated legacy soil maps for parts of Australia—chiefly Western Australia (WA) and the agricultural region of South Australia (SA). These activities have used the DSMART algorithm (Odgers *et al.* 2014*b*) to disaggregate the legacy soil maps and the PROPR algorithm (Odgers *et al.* 2015) to map the soil properties.

The spatial disaggregation and associated digital soil-property mapping work progressed concurrently with other nationwide digital soil-property mapping work by using only site data and spectroscopic estimates of soil properties (Viscarra Rossel *et al.* 2015), not as a duplication of effort but under the assumption that certain methods may work better in some parts of Australia than others. For example, it was supposed that soil-property estimates derived from the Cubist–kriging approach taken by Viscarra Rossel *et al.* (2015) would be less uncertain than derived from spatial disaggregation in areas where a reasonable density of point data existed. The soil-property estimates from the two sources were later merged by using a weighted-averaging approach to produce final soil-property estimates. Clifford and Guo (2015) describe other approaches potentially useful for model averaging.

This paper reports on the digital soil-property mapping that used spatially disaggregated, legacy soil-class maps in conjunction with the PROPR algorithm in WA and SA. We illustrate the work using clay content as an example.

## Methods

### *Study area and target soil property*

The study area consists of the part of Australia where legacy soil polygon maps have been spatially disaggregated using the DSMART algorithm, namely, the entirety of WA and the agricultural region of southern SA (Fig. 1). In the following sections, we briefly describe the spatial disaggregation of each state's legacy soil-class map coverage and the process by which the reference soil-property data were assembled. Finally, we present maps of clay content (per cent clay) estimates and associated uncertainty at the GlobalSoilMap depth intervals of 0–5, 5–15, 15–30, 30–60, 60–100 and 100–200 cm.

### *Soil-class probability rasters*

#### *The PROPR algorithm*

We used the PROPR algorithm (Odgers *et al.* 2014*a*, 2015) to generate maps of the target soil properties and their associated uncertainty by using the reference soil-property data and the set of soil-class probability rasters. The soil-property estimates are calculated as the weighted mean of the reference soil-property values, where the weights are the probabilities of occurrence of the relevant soil classes according to the following:

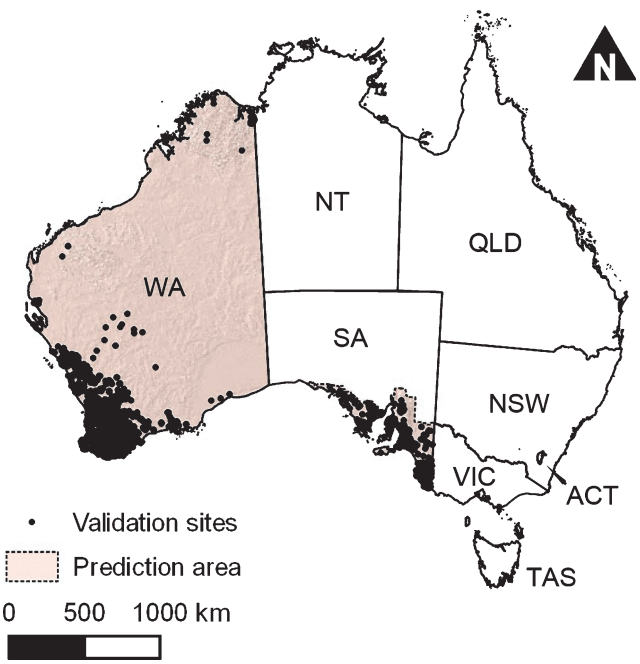


**Fig. 1.** Map of Australia showing PROPR prediction area (extent of spatially disaggregated soil coverage) and validation sites.

$$\mu* = \frac{\sum_{k=1}^{K} P_k g_k}{\sum_{k=1}^{K} P_k} \quad (1)$$

where $g_k$ is the reference soil-property value associated with soil class $k = 1, 2, 3, \ldots, k$ and $P_k$ is the estimated probability of occurrence of soil class $k$ at a given grid cell.

The uncertainty is indicated as the lower and upper limits of the 90% PI about the predicted central soil property value (GlobalSoilMap Science Committee 2013). The PI is an interval estimate of a quantity; a point estimate such as the weighted mean is expected to lie within the PI with a prescribed level of confidence (in our case, 90%). The PI is wider than the confidence interval (CI), which is an estimate of the accuracy of a regression (Shrestha and Solomatine 2006).

In order to estimate the PI, we need to have an estimate of the potential variability of the target soil property at the prediction locations. Given that knowledge of the within-soil-class variability of the target soil property may be incomplete—for example, if there are few observations of individuals belonging to the soil class—PROPR uses the triangular distribution to represent the target soil property distribution for each soil class. The triangular distribution is a simple distribution and requires three parameters, $a$, $b$ and $c$, corresponding to the lower limit, upper limit and mode of the distribution, respectively. The $c$ parameter does not need to be centrally located between the $a$ and $b$ parameters. The triangular distribution has been recommended for use in situations where the underlying distribution is unknown but values representing $a$, $b$ and $c$ may be known (Kotz and van Dorp 2004).

For each depth interval, we estimated the 90% PI limits by sampling proportionately from the triangular distributions of the soil classes that had a probability of occurrence >0 at the respective grid cell. The samples go into a new distribution of size $J$; thus, the number of samples drawn from each soil class is equal to:

$$j_k = P_k J \quad (2)$$

where $j_k$ is the number of samples drawn from the triangular distribution of soil class $k$ and $P_k$ is the probability of occurrence of soil class $k$ at the given grid cell. The 90% PI limits are then estimated as the 5th and 95th percentiles of this new distribution.

### *Assessment of maps of clay content*

We carried out two rounds of validation to assess the quality of the predictions of clay content. In each state, the first round of validation involved considering all available validation profiles at each depth interval regardless of their actual clay content. We then carried out a second round of validation in order to see whether the accuracy of different clay ranges was predicted differentially at different depth intervals. To do so, we grouped the validation sites into clay ranges roughly equivalent to texture grades.

In order to assess the performance of the predictions of clay content, we calculated the following validation statistics on the observed clay content from the available validation profiles and their corresponding predictions of clay content for each depth interval (first round) and depth interval–clay range combination (second round): root-mean-squared error (RMSE), mean error (ME), Lin's concordance correlation coefficient ($\rho_C$; Lin 1989), correlation coefficient ($r^2$), PI coverage probability (PICP), and the mean PI width. Methods of calculating these statistics, and their utility, are described in the remainder of this section.

In order to assess the precision of the clay predictions, we calculated the RMSE as:

$$\mathrm{RMSE} = \sqrt{\frac{\sum_{i=1}^{V} (\hat{z}_i - z_i)^2}{V}} \quad (3)$$

where $\hat{z}_v$ is the predicted clay content and $z_v$ the observed clay content of validation profile $i = 1, 2, 3, \ldots, V$ and $V$ is the number of validation profiles. The RMSE should be as small as possible.

In order to assess the degree of bias in the predictions of clay content, we calculated the ME as:

$$\mathrm{ME} = \frac{\sum_{i=1}^{V} (\hat{z}_i - z_i)}{V} \quad (4)$$

When ME is close to zero there is little bias in the predictions of clay content. A negative ME indicates that the predictions tend to be underestimated, and a positive ME indicates that the predictions tend to be overestimated.

We calculated $\rho_C$ in order to assess the degree of agreement of the data with the 1 : 1 line. Given two sets of samples denoted $m = 1, 2$, of size $n$ samples, $\rho_C$ is calculated as:

$$\rho_C = \frac{2S_{12}}{S_1^2 + S_2^2 + (\bar{Y}_2 - \bar{Y}_2)^2} \quad (5)$$

where the sample mean of sample set $m$ is calculated as $\overline{Y}_m = \frac{1}{n}\sum_{i=1}^{n} Y_{im}$, the sample variance of sample set $m$ is calculated as $S_j^2 = \frac{1}{n}\sum_{i=1}^{n} \left(Y_{im} - \overline{Y}_m\right)^2$ and the sample covariance between both sample sets is calculated as $S_{12} = \frac{1}{n}\sum_{i=1}^{n} \left(Y_{i1} - \overline{Y}_1\right)\left(Y_{i2} - \overline{Y}_2\right)$. In our case, the two sets of samples correspond to the observed and predicted clay contents for the given depth interval or depth interval–clay range combination. The $\rho_C$ ranges continuously from 0.0 to 1.0, and ideally the value should be as large as possible. Values of $\rho_C$ near 0 indicate that the agreement between observed and predicted data varies greatly from the 1 : 1 line, whereas values near 1.0 indicate that the agreement between observed and predicted data varies little from the 1 : 1 line.

The coefficient of determination, $r^2$, is calculated as:

$$r^2 = 1 - \frac{\sum_{i=1}^{V} (z_i - \hat{z}_i)^2}{\sum_{i=1}^{V} (z_i - \bar{z})^2} \quad (6)$$

where $\bar{z}$ is the average of the observed clay content at the given depth interval or depth interval–clay range combination. The $r^2$ measures the degree of linear relationship between the observed and predicted data but not how closely this relationship agrees with the 1 : 1 line. The $r^2$ ranges continuously from 0.0 to 1.0, and ideally, the value should be as large as possible: Values of $r^2$ close to 0 indicate a weak linear relationship between observed and predicted data, whereas values close to 1.0 indicate a strong linear relationship between observed and predicted data.

Caution is required when interpreting validation performance on the basis of $r^2$ alone because it is possible for the data to have

a strong agreement with the fitted line (high $r^2$) but low agreement with the 1 : 1 line (low $\rho_C$). For this, it is better to consider $r^2$ and $\rho_C$ in tandem and high values of both statistics are desirable.

The prediction-interval coverage probability, PICP, is the probability that an observed value falls within the PI, and is estimated as (adapted from Shrestha and Solomatine 2006):

$$\text{PICP} = \frac{1}{V}\sum_{i=1}^{V} q_i$$
$$q_i = \begin{cases} 1, \text{if } \text{PL}_{\text{L}i} \le z_i \le \text{PL}_{\text{U}i} \\ 0, \text{otherwise.} \end{cases} \quad (7)$$

where $\text{PL}_\text{L}$ and $\text{PL}_\text{U}$ are the lower and upper PI limits, respectively. Ideally, the value of PICP will be close to the nominal coverage probability, which in our case is 0.9 (i.e. 90%). PICP values greater than the nominal value indicate overestimation of the uncertainty (PIs are too wide); values less than the nominal value indicate underestimation of the uncertainty (PIs are too narrow).

The average prediction-interval width ($\overline{\text{PIW}}$) indicates the relative degree of uncertainty in the prediction of clay content; the wider the $\overline{\text{PIW}}$, the greater the average uncertainty and *vice versa*. Ideally, it will be as small as possible. It is calculated as:

$$\overline{\text{PIW}} = \frac{1}{V}\sum_{i=1}^{V} \text{PL}_{\text{U}i} - \text{PL}_{\text{L}i} \quad (8)$$

## Case studies

### *Western Australia*

The general distribution of soils in WA has been described in a soil-landscape hierarchical information system that stratifies the region by broad edaphic factors (Schoknecht *et al.* 2004). The soils of WA were mapped as 53 separate surveys and published at scales of 1 : 20 000–1 : 100 000 in agricultural and developing areas, 1 : 250–1 : 500 000 in adjacent rangelands, and 1 : 3 000 000 in the arid interior (Holmes *et al.* 2014). Map unit polygons provide the highest level of spatial detail and contain unmapped soil–landform relationships recorded as areal proportions. These polygons were spatially disaggregated by using the DSMART algorithm (Odgers *et al.* 2014*b*; Holmes *et al.* 2015), resulting in a set of 73 soil-class probability rasters, one for each of the Soil Groups in WA (Schoknecht and Pathan 2013). The Soil Group (e.g. 402: 'Grey deep sandy duplex') is roughly equivalent to the Suborder level of the Australian Soil Classification (Isbell 1996), Soil Taxonomy (Soil Survey Staff 1999) or the World Reference Base for Soil Resources (FAO 2014), and through trial and error was identified as the most appropriate level of detail for spatial disaggregation.

Soil Groups are horizon morphological descriptions developed to allow classification largely based on field description for agricultural purposes. For those Soil Groups distributed over large areas of WA, the measured physical and chemical properties tend to vary by physiographic zone ('soil-landscape zones' in Schoknecht *et al.* 2004). The available measurements contribute to a physiographic zone–Soil Group soil-properties model for the whole of WA. Although this is attributed at a more detailed level of the classification hierarchy than Soil Groups (i.e. Qualified Soil Groups), the knowledge of these properties is limited for all but the intensive agricultural region in the south-west of WA.

The reference soil property values required for PROPR (*a*, *b* and *c* parameters of the triangular distribution) were derived separately for each physiographic zone from the proportions of Qualified Soil Groups occurring in the physiographic zone (*c*) and the endmember Qualified Soil Groups occurring in each physiographic zone (*a* and *b*), as demonstrated in Table 1.

Georeferenced profile observations were used for validation although they were not well distributed spatially across WA (Fig. 1). Of the >50 000 profiles, 5% had laboratory-measured clay and the remainder had field estimates of texture class that were converted to a numeric mid-range value. For profiles and soil property values, depth-weighted averaging was used to generate values for GlobalSoilMap depth intervals, calculated separately for laboratory-measured and field observations. The data were compiled, prioritising laboratory analyses over field data, and missing values assigned to sites with neither measurement. For the six depth intervals, the number of validation sites available decreased from 50 671 at 0–5 cm to 11 548 at 100–200 cm.

### *South Australia*

#### *Spatial disaggregation*

The 61 'subgroup soils' (Hall *et al.* 2009; DEWNR 2014*a*) defined by the State Land and Soil Mapping Program (SLSMP) of SA and mapped at scales of 1 : 50 000–1 : 100 000 were identified as the most appropriate soil-type classes for disaggregation by the DSMART algorithm. These classes are morphologically defined soil types that capture the range of

**Table 1. Example of triangular distribution parameter calculation from Western Australian soil map unit database**

The areal proportion is the proportion of the Soil Group in a Zone that has a particular Qualifier. In this table, the Zone is Esperance Sandplain Zone (245) and the Soil Group is Grey shallow sandy duplex (404)

| Soil Group Qualifier | Areal proportion | 15–30 cm model clay (% clay) | Triangular distribution parameter |
|---|---|---|---|
| ACD (good acid subsoil) | 0.01 | 8 (max) | Upper limit = *b* |
| NEU (good neutral subsoil) | 0.40 | 4 (min) | Lower limit = *a* |
| PSS (poor subsoil) | 0.45 | 4 | |
| RKM (rock substrate) | 0.13 | 6 | |
| SSS (saline subsoil) | 0.00 | 4 | |
| | Area-wt mean: | 4.3 | Mode = *c* |

variation in soils across the agricultural zone of southern SA. Subgroup soil-class names are associated with alphanumeric code names (e.g. 'A1' refers to a highly calcareous sandy loam) and arranged into a hierarchical naming system. At the higher hierarchical level, 'soil groups' are described by a single letter code (e.g. 'A' refers to calcareous soils), whereas at lower hierarchical level, the subgroup soils are classified into regional variants (e.g. 'A1B' refers to a highly calcareous loam over Padthaway formation sediments). These regional variants correspond to regionally representative soil-profile concepts that underpin soil-landscape mapping of SA in a form that has been translated to meet the specifications of McKenzie *et al*. (2012), otherwise known as 'national-format' soil-mapping datasets (DEWNR 2014*b*). Like the Soil Groups of WA, the subgroup soils of SA are a state-based classification developed to suit local conditions. There is no link with the Soil Group classification system of WA.

### *Reference soil-property data*

South Australia's regional variant soils were identified as the most appropriate data source to provide soil-property values (e.g. soil pH, clay content) and the within-soil-class variability for each of the 61 subgroup soils. The regional variants of the subgroup soils are representative soil profiles with expert-derived estimates (based on real site data) for a range of quantitative functional soil properties. At the time of writing, 1529 regional variants or representative profiles have been described, spanning the 61 subgroup soil classes, in a form to meet the specifications of the Australian Soil Resource Information System (McKenzie *et al.* 2012).

Expert-based assessments were made of both the representative profile properties and their areal proportion within soil-landscape map units, based on ~1100 detailed soil characterisation sites (excavated pits with field description and laboratory analyses), 25 000 less detailed sites (hand-auger holes with limited field assessment) and 15 years of experience of a field-survey team via the SLSMP (Hall *et al.* 2009).

For the example of surface clay content, the number of regional variants per subgroup soil averages ~24, with a range of 3–82 (excluding peats, which have no clay data); however, the available data vary with different soil properties and depth ranges, with typically fewer regional variant profile estimates available deeper in the profile.

Equal-area smoothing splines were applied to the regional variant data in order to obtain estimates of clay content at the GlobalSoilMap depth intervals. For each depth interval, the area-weighted mean clay content was calculated for each subgroup soil and treated as the reference value for the respective subgroup soil. The *a* and *b* parameters of the triangular distribution were treated as the minimum and maximum regional variant clay content within each subgroup soil class. The *c* parameter of the triangular distribution was assumed equal to the area-weighted mean clay content for each subgroup soil.

In SA, 908 sites were available for validation (Fig. 1).

## Results and discussion

Across most of the landscape, clay content tends to increase down the soil profile but can decline again towards the lowest depth intervals (Fig. 2). This is consistent with a general expectation for many soils to exhibit a zone of clay accumulation below which textures can coarsen as the limit of clay illuviation is exceeded and many substrate materials are not yet sufficiently weathered and broken down to finer textures. The trend is most marked in the south-west of WA and south-eastern SA but is less evident, for example, in parts of the central north of WA. The degree of uncertainty, as expressed by the width of the 90% PI, also increases down the soil profile (Fig. 3). The increase in uncertainty down the soil profile is greatest in parts of the arid central east and the south-west of WA and not as strong in the north of WA near Broome and the western part of the agricultural region in SA. An example of the maps of the PI limits alongside the weighted mean for the 0–5 cm depth interval is presented in Fig. 4.

On average, soils in the agricultural region of SA contain more clay than soils of WA, although the average uncertainty in the clay estimates from SA is greater than that of the clay estimates from WA in the top four depth intervals. Although on average the clay estimates from WA have less uncertainty than the estimates from SA, the widths of the 90% PIs in WA are more variable than SA in all depth intervals except for 100–200 cm.

### *Validation*

The results of the first round of validation are presented in Table 2 for WA and Table 3 for SA. Some of the differences between these statistics may be due to the large difference in the number of validation observations available and the potential that many of the data from WA are lower quality (being estimated from field texture). The values of $\rho_C$ were $\geq$0.3 at all depth intervals in both states (with a maximum of 0.518 at 100–200 cm in WA), indicating a weak linear trend between predicted and observed clay contents. The values we observed are within the range recorded in the literature (e.g. Malone *et al.* 2009), although some researchers have reported $\rho_C > 0.7$ in their analyses (e.g. Lawes *et al.* 2009; Huang *et al.* 2014; Kidd *et al.* 2014). The fit to the 1 : 1 line was greater at the depth intervals 0–5 and 100–200 cm, where most soils in WA are sand or clay, respectively, than in the middle of the profile. The middle intervals, where predictions were poorer, are where the range of clay is greatest. A depth-related trend was more subtle in SA. The $r^2$ values indicate a significant variance around the *fitted* line for each depth interval, particularly so in SA. In both states, RMSE was lowest at 0–5 cm and tended to increase down the profile. Considering that the range of clay in a single field texture class is usually 5–10% (McDonald and Isbell 2009), these results indicate that the predictions are likely accurate to within one or two field texture grades (Table 4). In both states, the trend in ME was subtle across depth intervals, being <5% clay above or below zero in all cases. The $\overline{\text{PIW}}$ tended to increase with clay content to a maximum at 60–100 cm (WA) and 30–60 cm (SA). This was equivalent to the range of clay content between several field texture grades (Table 4). Even so, the proportion of validation sites whose observed clay content was within the 90% PI (PICP) was always less than the expected 0.9, indicating that the uncertainty was underestimated (more severely in SA than WA).

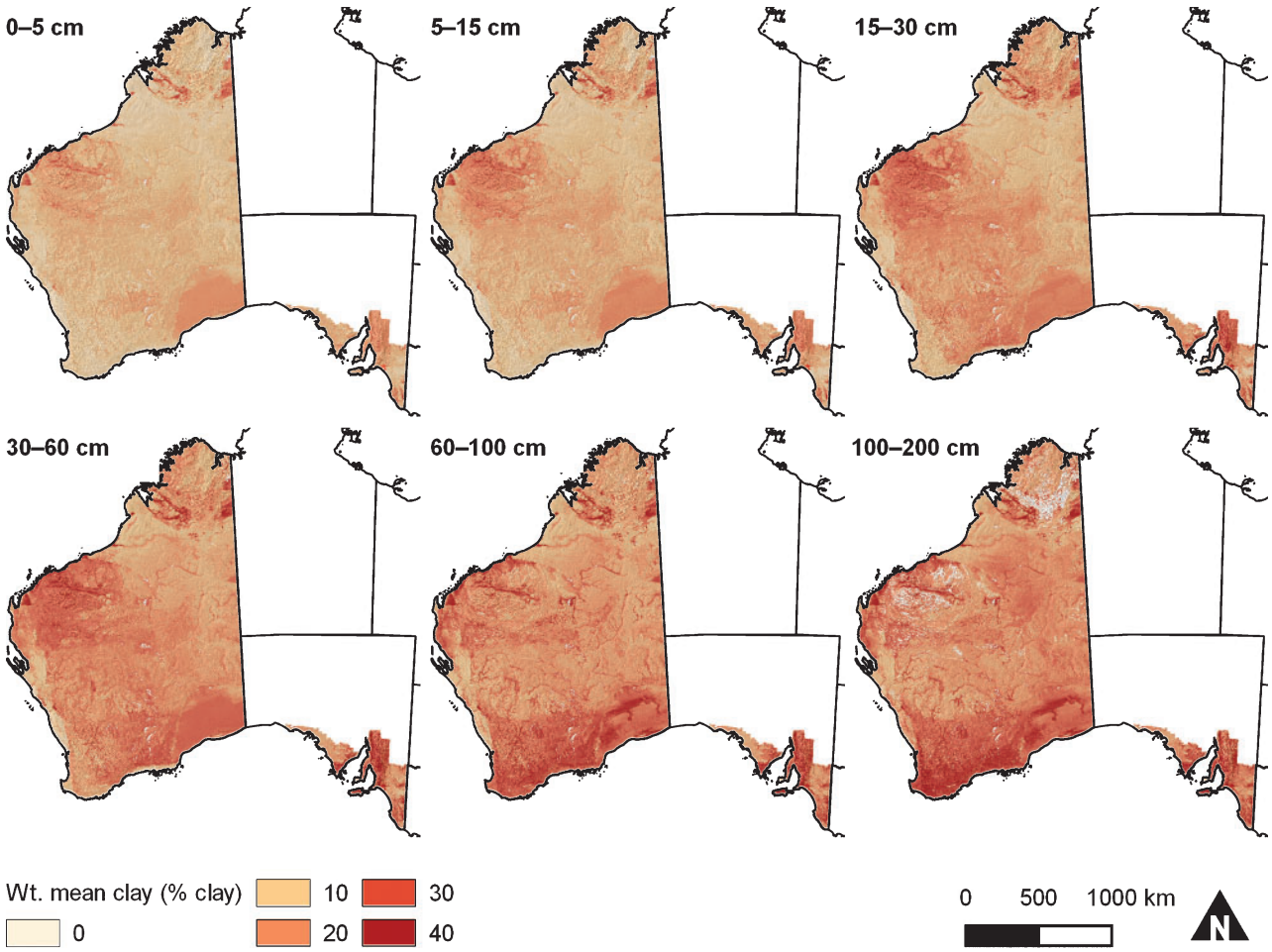


**Fig. 2.** Maps of weighted-mean clay content (% clay) for the six depth intervals.

The results of the second round of validation are presented in Table 5 for WA and Table 6 for SA.

The validation statistics ($\rho_C$ and $r^2$) for the various ranges of clay content were poorer than for the global validations. Values of $\rho_C$ and $r^2$ were generally of the same magnitude in both states. In WA, $\rho_C$ was highest in the clay range 5–<10% in the depth intervals 0–5 and 5–15 cm, but at depth was highest in the clay range 35–<50%, with a secondary peak at 20–<30% clay. In SA, $\rho_C$ followed a similar trend although the maximum $\rho_C$ above 15 cm in the profile was found in the clay range 10–<20%.

In both states, the clay range with the minimum RMSE became more clayey with depth. In WA, RMSE was lowest in soils with 0–<5% and 5–<10% clay (at 0–5 and 5–15 cm), 10–<20% clay (at 15–30 and 30–60 cm), and 20–<30% and 30–<35% clay (at 60–100 and 100–200 cm). In SA, the clay range with the minimum RMSE was more clayey than in WA for the same depth interval above 60 cm in the soil profile. The RMSE was lowest in soils with 10–<20% clay (at 0–5 and 5–15 cm), 20–<30% clay (at 15–30 and 30–60 cm), and 30–35% clay (at 60–100 and 100–200 cm). Minimum RMSEs were ≤10% clay in all cases, which is within one or two field texture classes. The highest RMSEs were usually found in the 50–100% clay range and could be up to 39% clay.

In WA and SA, the texture grades where the predictions were the least biased (ME closest to zero) were the same as those that had the minimum RMSE, except for the depth interval 60–100 cm in WA, where the predictions in the clay range 20–<30% (loams) were the least biased. In both states at all depth intervals, predictions were always the most biased in soils with the highest clay content, although the least biased predictions were not in soils with the lowest clay content. As observed clay content increased, the predicted clay content was increasingly underestimated (negative ME); the degree of underestimation is particularly severe for soils with 35–100% clay (light, medium and heavy clays) above 30 cm in the soil profile in both states, particularly in WA. On the other hand, the clay content of soils with low observed clay content is routinely overestimated.

The PICP varied considerably across states, depth intervals and texture grades. At a given depth interval, PICP tended to approach 0.9 for only one or two clay ranges; the PICP of the other clay ranges was typically <0.9, indicating underestimation of the uncertainty (the PIs should be wider). The best-case PICPs were better than the PICPs recorded for the first-round validation described above. The clay content of best-case PICP tended to increase with depth in the profile. The uncertainty of some clay

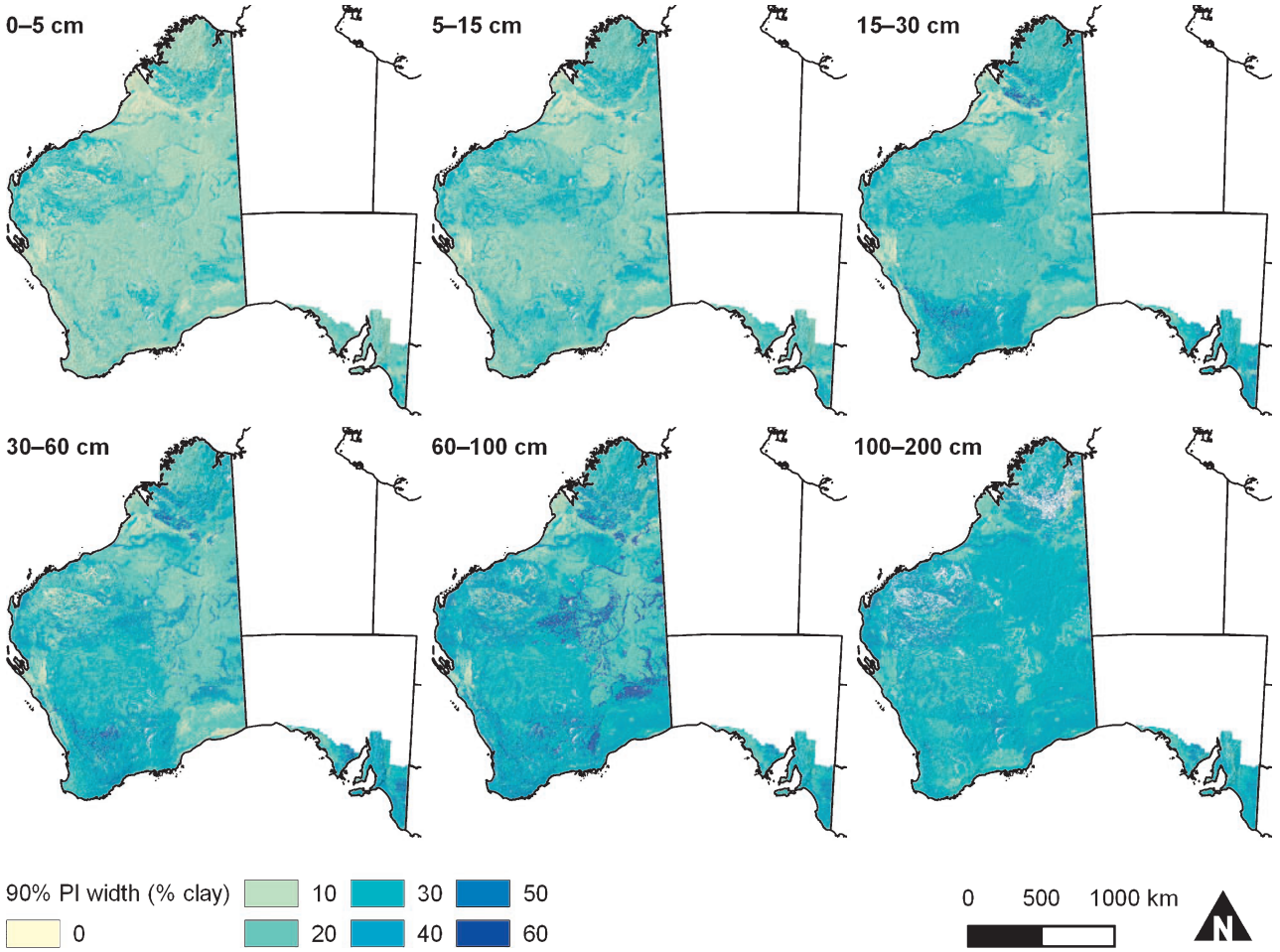


**Fig. 3.** Maps of the width of the 90% prediction interval (PI) around the weighted mean clay estimates. A low prediction interval width indicates low uncertainty and *vice versa*.

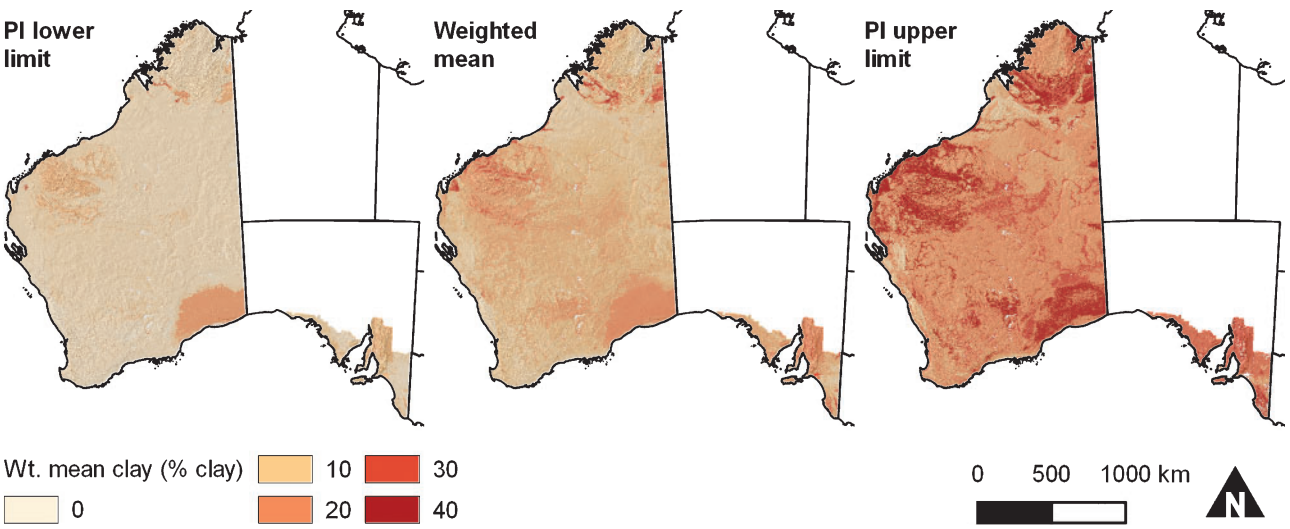


**Fig. 4.** Maps of 0–5 cm clay content (% clay) showing, from left to right, the lower prediction interval limit, weighted mean and upper prediction interval (PI) limit.

**Table 2. Summary of validation of Western Australian clay maps**

$\rho_C$, Lin's concordance correlation coefficient; $r^2$, coefficient of determination; RMSE, root-mean-square error; ME, mean error; PICP, prediction interval coverage probability; $\overline{\text{PIW}}$, mean prediction interval width; *V*, number of validation sites used to calculate the statistics

| Depth interval (cm) | $\rho_C$ | $r^2$ | RMSE (% clay) | ME (% clay) | PICP | $\overline{\text{PIW}}$ (% clay) | *V* |
|---|---|---|---|---|---|---|---|
| 0–5 | 0.421 | 0.343 | 8.4 | –2.6 | 0.838 | 15.6 | 50614 |
| 5–15 | 0.343 | 0.260 | 11.2 | –4.1 | 0.800 | 20.0 | 50486 |
| 15–30 | 0.318 | 0.202 | 15.2 | –4.6 | 0.771 | 27.6 | 45827 |
| 30–60 | 0.398 | 0.286 | 15.4 | –4.7 | 0.748 | 31.7 | 42203 |
| 60–100 | 0.500 | 0.338 | 14.9 | 1.1 | 0.767 | 35.9 | 28466 |
| 100–200 | 0.518 | 0.394 | 15.0 | 4.3 | 0.504 | 29.6 | 11398 |

**Table 3. Summary of validation of South Australian clay maps**

$\rho_C$, Lin's concordance correlation coefficient; $r^2$, coefficient of determination; RMSE, root-mean-square error; ME, mean error; PICP, prediction interval coverage probability; $\overline{\text{PIW}}$, mean prediction interval width; *V*, the number of validation sites used to calculate the statistics

| Depth interval (cm) | $\rho_C$ | $r^2$ | RMSE (% clay) | ME (% clay) | PICP | $\overline{\text{PIW}}$ (% clay) | *V* |
|---|---|---|---|---|---|---|---|
| 0–5 | 0.364 | 0.241 | 12.1 | 0.9 | 0.575 | 21.4 | 908 |
| 5–15 | 0.361 | 0.216 | 13.5 | –1.2 | 0.654 | 25.0 | 897 |
| 15–30 | 0.300 | 0.148 | 17.3 | –3.4 | 0.703 | 33.4 | 837 |
| 30–60 | 0.349 | 0.177 | 18.4 | –2.2 | 0.691 | 36.6 | 744 |
| 60–100 | 0.340 | 0.169 | 17.4 | –0.2 | 0.671 | 33.8 | 586 |
| 100–200 | 0.300 | 0.143 | 17.0 | 3.8 | 0.679 | 33.9 | 321 |

**Table 4. Texture grades generalised from McDonald and Isbell (2009) for examining the performance of the maps of clay content at different clay contents**

| Generalised texture grade | Range in clay content |
|---|---|
| Sands | 0–<5% |
| Loamy/clayey sands | 5–<10% |
| Sandy loams | 10–<20% |
| Loams | 20–<30% |
| Clay loams | 30–<35% |
| Light/medium clays | 35–<50% |
| Heavy clays | 50–100% |

ranges, such as the 50–100% clays in WA and SA, was consistently underestimated regardless of depth interval, whereas the PICP of other clay ranges, such as the 10–<20% clays in WA and the 20–<30% clays in SA, was consistently closer to 0.9 across all depth intervals.

In both states, the $\overline{\text{PIW}}$ indicated that uncertainty tended to increase with depth across all generalised texture grades, although in WA, the uncertainty was highest in the 60–100 cm depth interval where the texture-contrast layer commonly occurs. In WA, uncertainty tended to increase with increasing clay content in the depth intervals 0–5 and 5–15 cm; however, the trend was more subtle in the rest of the profile. The uncertainty actually tended to decrease with increasing clay content at 100–200 cm depth, so that the 50–100% clay estimates had the lowest uncertainty. Trends in the SA maps were less clear, although there was variation between texture grades at each depth interval. The uncertainty in the SA maps tended to be slightly greater than for the WA maps at most depth interval–texture grade pairs, except for the 60–100 cm depth interval where the SA predictions had slightly less uncertainty.

We noticed that the PI width relative to the mean (midpoint) of the clay ranges was much greater for observations with very low clay than with high clay (~10× compared with 0.5×). It is not clear from the validation statistics why this is the case, but it probably originates in the often wide range of soils (with respect to clay content) predicted in a grid cell by DSMART. The wide range in clay content is more significant when the bias is also large, such as in predictions on soils with very low clay content at depth. To test this, we segregated two contrasting segments of the validation data from WA. Both segments had very sandy surface observations (very low clay content) but one where sands predominate at depth (deep sands important; DSi) whereas the other had moderate to high clay content at depth (deep sands rare; DSr). This segregation comes from area-weighted averages of soil classes in soil-landscape zones, that is, different areas of WA.

Table 7 reveals the contrast in bias (ME) for these segments of data for the greater depth intervals. In areas with predominantly deep sands, the bias for soils with sand at depth (i.e. low clay content at depth) was generally <10% clay. On the other hand, in areas with predominantly high clay content at depth, the clay prediction bias for soils with sand at depth was typically >20% clay. Notably, in this case, there was a better prediction (less bias) of high clay at depth. In Fig. 5, the mean predicted clay contents of the most common clay ranges found in DSi and DSr are closer to the 1 : 1 line than the mean clay contents of the other ranges of clay content. This suggests that where significant under- or over-prediction occurs,

**Table 5. Summary of validation of Western Australian clay maps by clay content**

$\rho_C$, Lin's concordance correlation coefficient; $r^2$, coefficient of determination; RMSE, root-mean-square error; ME, mean error; PICP, prediction interval coverage probability; $\overline{\text{PIW}}$, mean prediction interval width; *V*, number of validation sites used to calculate the statistics

| Depth interval (cm) | Clay range (%) | $\rho_C$ | $r^2$ | RMSE (% clay) | ME (% clay) | PICP | $\overline{\text{PIW}}$ (% clay) | *V* |
|---|---|---|---|---|---|---|---|---|
| 0–5 | 0–<5 | 0.081 | 0.047 | 3.4 | 2.1 | 0.865 | 12.6 | 11385 |
| | 5–<10 | 0.124 | 0.059 | 3.0 | 1.0 | 0.966 | 15.4 | 21668 |
| | 10–<20 | 0.043 | 0.027 | 6.6 | –5.4 | 0.882 | 17.0 | 11644 |
| | 20–<30 | 0.001 | 0.000 | 14.1 | –13.4 | 0.321 | 18.0 | 2799 |
| | 30–<35 | 0.000 | 0.003 | 19.2 | –18.4 | 0.327 | 20.1 | 1043 |
| | 35–<50 | 0.023 | 0.059 | 26.1 | –24.8 | 0.096 | 22.3 | 1361 |
| | 50–100 | 0.016 | 0.030 | 35.6 | –33.64 | 0.000 | 21.3 | 714 |
| 5–15 | 0–<5 | 0.058 | 0.030 | 3.9 | 2.3 | 0.858 | 15.8 | 11213 |
| | 5–<10 | 0.105 | 0.057 | 3.8 | 1.7 | 0.962 | 19.6 | 17804 |
| | 10–<20 | 0.094 | 0.033 | 6.1 | –4.0 | 0.935 | 21.4 | 10594 |
| | 20–<30 | 0.000 | 0.071 | 15.1 | –13.8 | 0.536 | 22.6 | 4929 |
| | 30–<35 | 0.000 | 0.082 | 21.7 | –20.8 | 0.262 | 22.8 | 2349 |
| | 35–<50 | 0.011 | 0.018 | 27.2 | –26.0 | 0.196 | 25.4 | 2570 |
| | 50–100 | 0.020 | 0.046 | 36.9 | –34.8 | 0.000 | 23.9 | 1027 |
| 15–30 | 0–<5 | 0.026 | 0.022 | 7.2 | 4.7 | 0.848 | 22.3 | 12095 |
| | 5–<10 | 0.047 | 0.046 | 7.2 | 4.9 | 0.950 | 27.0 | 10719 |
| | 10–<20 | 0.100 | 0.026 | 6.0 | –0.1 | 0.961 | 29.0 | 6683 |
| | 20–<30 | 0.011 | 0.002 | 10.5 | –8.1 | 0.863 | 30.5 | 5630 |
| | 30–<35 | 0.000 | 0.002 | 15.3 | –13.7 | 0.707 | 31.4 | 1811 |
| | 35–<50 | 0.013 | 0.013 | 23.7 | –22.2 | 0.408 | 33.5 | 5528 |
| | 50–100 | 0.023 | 0.143 | 38.5 | –37.2 | 0.026 | 29.5 | 3361 |
| 30–60 | 0–<5 | 0.022 | 0.027 | 8.8 | 6.4 | 0.782 | 24.9 | 8823 |
| | 5–<10 | 0.026 | 0.035 | 9.9 | 8.0 | 0.916 | 30.4 | 7330 |
| | 10–<20 | 0.077 | 0.021 | 7.2 | 3.2 | 0.946 | 32.8 | 5343 |
| | 20–<30 | 0.035 | 0.008 | 8.4 | –5.1 | 0.939 | 33.9 | 6182 |
| | 30–<35 | 0.000 | 0.000 | 12.6 | –10.4 | 0.831 | 34.1 | 2160 |
| | 35–<50 | 0.019 | 0.015 | 20.4 | –18.8 | 0.594 | 35.9 | 8675 |
| | 50–100 | 0.023 | 0.061 | 32.5 | –30.8 | 0.037 | 34.5 | 3690 |
| 60–100 | 0–<5 | 0.014 | 0.037 | 14.9 | 11.6 | 0.690 | 32.9 | 6196 |
| | 5–<10 | 0.004 | 0.003 | 16.2 | 13.6 | 0.867 | 35.7 | 4853 |
| | 10–<20 | 0.038 | 0.029 | 12.6 | 9.7 | 0.937 | 37.0 | 2631 |
| | 20–<30 | 0.051 | 0.011 | 7.8 | 2.1 | 0.975 | 37.3 | 3608 |
| | 30–<35 | 0.000 | 0.000 | 7.7 | –2.9 | 0.969 | 37.6 | 1311 |
| | 35–<50 | 0.037 | 0.011 | 13.0 | –10.3 | 0.786 | 37.8 | 6890 |
| | 50–100 | 0.021 | 0.017 | 24.3 | –22.1 | 0.227 | 34.8 | 2977 |
| 100–200 | 0–<5 | 0.000 | 0.000 | 17.7 | 15.2 | 0.081 | 30.0 | 2875 |
| | 5–<10 | 0.008 | 0.010 | 17.0 | 14.5 | 0.454 | 31.1 | 1928 |
| | 10–<20 | 0.031 | 0.021 | 13.5 | 10.6 | 0.827 | 31.6 | 1108 |
| | 20–<30 | 0.051 | 0.018 | 9.0 | 4.7 | 0.978 | 30.1 | 1385 |
| | 30–<35 | 0.000 | 0.000 | 7.3 | –0.4 | 0.969 | 29.8 | 424 |
| | 35–<50 | 0.065 | 0.018 | 10.3 | –7.3 | 0.735 | 28.8 | 2448 |
| | 50–100 | 0.044 | 0.044 | 20.3 | –18.2 | 0.126 | 25.8 | 1230 |

it may be associated with small proportions of the validation data and thus is not a reflection of the overall result.

## Discussion

The spatial pattern of clay content depicted by the maps (Fig. 2) is generally plausible when compared with distributions mapped previously (cf. the Australian Soil Resource Information System, www.asris.csiro.au). Although not a rigorous measure of map quality, this suggests that the DSMART predictions broadly concur with existing pedological knowledge and are able to produce a general picture of the spatial distribution of clay content in WA and southern SA. Methodology, availability of validation data, and difficulty of incorporating known soil-class–landform relationships may be responsible for the apparent poor quality of the global validation. As others have suggested (e.g. Bishop *et al.* 2012), a closer examination on a regional basis (e.g. the deep sands *v.* sands over clays in Table 7) may show differentially better performance.

The application of digital soil mapping techniques to the spatial prediction of clay content is quite common in the literature. Studies are often conducted at the field or farm

**Table 6. Summary of validation of South Australian clay maps by clay content**

$\rho_C$, Lin's concordance correlation coefficient; $r^2$, coefficient of determination; RMSE, root-mean-square error; ME, mean error; PICP, prediction interval coverage probability; $\overline{\text{PIW}}$, mean prediction interval width; $V$, number of validation sites used to calculate the statistics

| Depth interval (cm) | Clay range (%) | $\rho_C$ | $r^2$ | RMSE (% clay) | ME (% clay) | PICP | $\overline{\text{PIW}}$ (% clay) | $V$ |
|---|---|---|---|---|---|---|---|---|
| 0–5 | 0–<5 | 0.016 | 0.019 | 11.1 | 9.8 | 0.274 | 21.6 | 212 |
| | 5–<10 | 0.027 | 0.031 | 9.4 | 8.2 | 0.524 | 20.6 | 208 |
| | 10–<20 | 0.106 | 0.017 | 5.1 | 1.8 | 0.955 | 20.2 | 242 |
| | 20–<30 | 0.000 | 0.000 | 8.8 | –6.3 | 0.821 | 22.1 | 112 |
| | 30–<35 | 0.029 | 0.106 | 12.2 | –10.8 | 0.529 | 23.5 | 34 |
| | 35–<50 | 0.037 | 0.065 | 20.8 | –19.3 | 0.206 | 22.7 | 68 |
| | 50–100 | 0.000 | 0.019 | 34.4 | –32.5 | 0.000 | 25.4 | 32 |
| 5–15 | 0–<5 | 0.007 | 0.004 | 11.4 | 9.7 | 0.417 | 25.0 | 175 |
| | 5–<10 | 0.000 | 0.000 | 9.4 | 7.9 | 0.610 | 24.1 | 154 |
| | 10–<20 | 0.111 | 0.024 | 6.2 | 2.5 | 0.948 | 24.1 | 229 |
| | 20–<30 | 0.077 | 0.026 | 8.6 | –5.4 | 0.931 | 25.4 | 160 |
| | 30–<35 | 0.024 | 0.035 | 13.5 | –10.6 | 0.532 | 24.3 | 47 |
| | 35–<50 | 0.002 | 0.000 | 21.4 | –19.3 | 0.326 | 26.2 | 89 |
| | 50–100 | 0.000 | 0.017 | 36.8 | –34.2 | 0.000 | 28.4 | 43 |
| 15–30 | 0–<5 | 0.009 | 0.011 | 17.1 | 14.7 | 0.561 | 33.4 | 114 |
| | 5–<10 | 0.000 | 0.003 | 13.4 | 11.6 | 0.744 | 32.5 | 78 |
| | 10–<20 | 0.056 | 0.015 | 9.3 | 5.5 | 0.938 | 33.7 | 146 |
| | 20–<30 | 0.086 | 0.020 | 8.1 | –2.5 | 0.953 | 32.5 | 192 |
| | 30–<35 | 0.000 | 0.001 | 10.8 | –6.2 | 0.925 | 35.2 | 67 |
| | 35–<50 | 0.049 | 0.041 | 17.5 | –14.7 | 0.575 | 33.5 | 134 |
| | 50–100 | 0.000 | 0.021 | 34.8 | –31.9 | 0.066 | 33.8 | 106 |
| 30–60 | 0–<5 | 0.000 | 0.016 | 21.8 | 18.7 | 0.338 | 35.2 | 74 |
| | 5–<10 | 0.020 | 0.061 | 15.8 | 13.9 | 0.654 | 34.0 | 52 |
| | 10–<20 | 0.037 | 0.016 | 14.0 | 10.3 | 0.840 | 35.9 | 106 |
| | 20–<30 | 0.021 | 0.002 | 11.2 | 4.1 | 0.912 | 36.6 | 136 |
| | 30–<35 | 0.000 | 0.017 | 10.0 | –1.8 | 0.960 | 36.9 | 50 |
| | 35–<50 | 0.078 | 0.026 | 12.8 | –7.8 | 0.885 | 38.0 | 183 |
| | 50–100 | 0.000 | 0.021 | 30.3 | –27.1 | 0.224 | 37.7 | 143 |
| 60–100 | 0–<5 | 0.000 | 0.068 | 22.8 | 20.2 | 0.222 | 32.6 | 54 |
| | 5–<10 | 0.003 | 0.001 | 15.9 | 14.3 | 0.679 | 34.1 | 28 |
| | 10–<20 | 0.035 | 0.021 | 14.8 | 11.7 | 0.726 | 34.3 | 84 |
| | 20–<30 | 0.043 | 0.011 | 11.3 | 6.6 | 0.824 | 33.3 | 119 |
| | 30–<35 | 0.006 | 0.000 | 9.5 | 2.4 | 0.964 | 33.3 | 55 |
| | 35–<50 | 0.131 | 0.055 | 10.6 | –6.1 | 0.922 | 33.7 | 141 |
| | 50–100 | 0.000 | 0.040 | 28.9 | –25.3 | 0.190 | 32.6 | 105 |
| 100–200 | 0–<5 | 0.000 | 0.020 | 21.4 | 19.6 | 0.121 | 33.9 | 33 |
| | 5–<10 | 0.001 | 0.000 | 21.7 | 19.7 | 0.370 | 36.8 | 27 |
| | 10–<20 | 0.013 | 0.006 | 15.9 | 13.7 | 0.776 | 35.7 | 58 |
| | 20–<30 | 0.058 | 0.032 | 11.2 | 8.4 | 0.899 | 34.4 | 69 |
| | 30–<35 | 0.056 | 0.038 | 9.0 | 1.1 | 1.000 | 32.9 | 26 |
| | 35–<50 | 0.015 | 0.001 | 11.1 | –6.0 | 0.901 | 35.4 | 71 |
| | 50–100 | 0.000 | 0.123 | 29.0 | –24.9 | 0.189 | 31.4 | 37 |

scale in support of hydrological analyses or crop production (e.g. Triantafilis *et al.* 2001; Zhao *et al.* 2009), and others have been carried out at regional (e.g. Gallichand and Marcotte 1993; Lamsal and Mishra 2010; Gomez *et al.* 2012) and even continental scales (e.g. Henderson *et al.* 2005). Often, they are carried out in conjunction with soil electromagnetic investigations (e.g. Triantafilis and Lesch 2005; De Benedetto *et al.* 2012). Some authors made spatial predictions of clay content and validated them at several depths in the soil profile (e.g. Odeh *et al.* 2006); however, they do not appear to have validated their predictions at sub-ranges of observed clay content as presented here. Explicit spatial representation of the error or uncertainty in clay predictions also appears to be rare (e.g. Hong *et al.* 2012).

The methodological issues that Odgers *et al.* (2015) identified, that is, the influence of soil classes with very low probabilities of occurrence and the choice of distribution used to represent the within-soil-class variability in clay content, may play a role in the results we obtained. Sampling from a triangular distribution with the same range as a normal distribution tends to lead to higher representation of the tails than occurs if the normal distribution is sampled; this

**Table 7. Mean error by depth interval by clay range for areas in Western Australia with predominantly sandy surface soils but contrasting clay content at depth**

DSi soils are predominantly sandy at depth; DSr soils are predominantly clayey at depth. Positive mean errors denote over-prediction of clay content; negative mean errors denote under-prediction of clay content

| Segment | Depth interval (cm) | 0–<5% | 5–<10% | 10–<20% | 20–<30% | 30–<35% | 35–<50% | 50–100% |
|---|---|---|---|---|---|---|---|---|
| DSi | 0–5 | 0.7 | –0.7 | –6.8 | –15.8 | –24.8 | –29.5 | –48.2 |
| | 5–15 | 0.3 | –0.6 | –5.5 | –14.9 | –23.4 | –27.8 | –46.0 |
| | 15–30 | 1.0 | 0.2 | –4.0 | –12.1 | –18.5 | –28.1 | –43.6 |
| | 30–60 | 2.4 | 1.7 | –3.4 | –9.0 | –17.0 | –24.6 | –39.7 |
| | 60–100 | 5.9 | 4.5 | –1.5 | –8.8 | –15.2 | –18.7 | –32.9 |
| | 100–200 | 12.7 | 9.8 | 3.4 | –4.3 | –10.2 | –16.5 | –27.3 |
| DSr | 0–5 | 3.0 | 0.7 | –6.6 | –15.4 | –21.2 | –28.0 | –39.0 |
| | 5–15 | 3.7 | 1.3 | –5.4 | –14.2 | –20.6 | –27.8 | –37.9 |
| | 15–30 | 9.3 | 6.1 | –0.6 | –7.5 | –13.9 | –20.1 | –31.6 |
| | 30–60 | 13.4 | 11.2 | 4.2 | –2.6 | –8.7 | –15.6 | –25.9 |
| | 60–100 | 22.7 | 18.9 | 12.8 | 5.9 | 0.9 | –5.2 | –17.3 |
| | 100–200 | 27.1 | 24.5 | 17.6 | 9.9 | 4.7 | –2.9 | –14.9 |

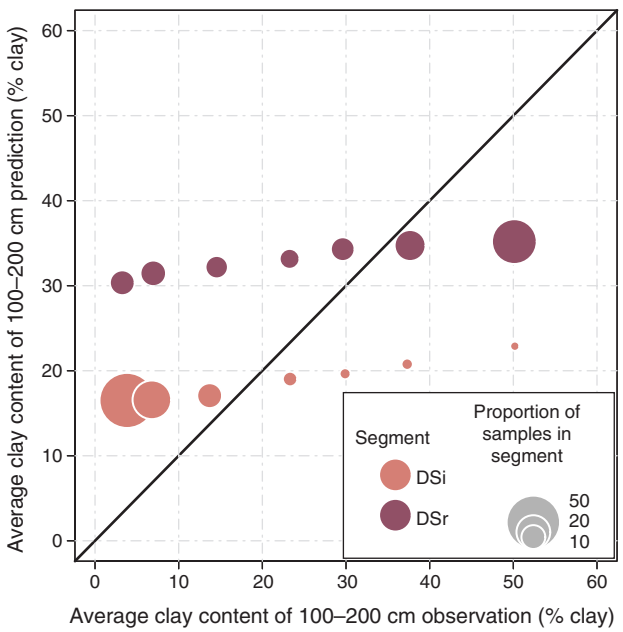


**Fig. 5.** Plot showing the average clay content of observations *v.* average clay content of predictions for each range of clay content for the 100–200 cm DSr and DSi segments of the Western Australian validation data. Diagonal solid line is the 1 : 1 line. Circle area is proportional to the proportion of validation sites in each clay range within each segment of data.

should lead to higher, rather than lower, uncertainty. On the other hand, the fact that the uncertainty was often underestimated appears to discount the role of the triangular distribution in our case.

Although the soils that DSMART predicts tend to be the more common soils, the confidence with which it predicts them is highly variable and is closely related to the degree of purity of soils within the mapping unit (Holmes *et al.* 2015). This uncertainty is carried forward into the uncertainty computed by PROPR.

Limited site data were available to both characterise the within-soil-class variability and validate the maps of clay. Confounding this is that available data may be biased. Holmes *et al.* (2015) demonstrated that in WA, data on the rare soils were relatively more abundant than data on the common soils. Thus, it is clear that in WA, site data are not representative for the whole landscape and certain texture grades, although representation by texture grade improves with depth in the profile. In addition, there is imprecision in the validation data from WA because the clay content of most soils was estimated from field texture. In SA, the representation is more uniform in landscape space and attribute space but the number of sites available is relatively low.

Expert knowledge had a big part to play in the clay maps presented here. The probability rasters produced by DSMART itself are a representation of the expert knowledge in map-unit polygons and their component proportions. Similarly, the clay inferences and uncertainty generated by PROPR were based on such knowledge because site measurements were limited. Where site data are limited in landscape space and attribute space, it may be reasonable to assume that expert knowledge may be incomplete. On the one hand, experts may have a reasonable idea of the typical clay content of a particular soil class but they may over- or underestimate its within-class variability. On the other hand, if they are more familiar with soils that have a particular range of clay content than with other soils, they may over- or underestimate the typical clay content of those soil classes outside their common range of experience. Evidence for the former situation is difficult to quantify; as a proxy PICP does not correlate very well with the number of observations available across generalised texture grades for particular depth intervals in either state. Evidence for the latter situation could be the variation in the degree of bias as expressed by the mean error at different generalised texture grades and depth intervals in Tables 5 and 6.

The limitations and deficiencies outlined here may influence the outcome. On the one hand, the within-soil-class variability may be underestimated in some soil classes because of sampling bias or a limited number of observations; on the other hand, validation could be biased if certain soil classes are over- or under-represented in the validation dataset. Either situation could lead to suboptimal PICP values.

As it stands, our PICP results are similar to those reported by others, although use of the PICP in the soil literature seems rare. For example, using a different technique, Helmick *et al*. (2014) generated 95% PIs for GlobalSoilMap products for a range of soil properties for the six standard depth intervals in the contiguous United States and observed PICPs in the range of 0.5–1.0 when the validation was stratified by Soil Order, temperature regime or moisture regime. Malone *et al*. (2011) reported PICPs of 0.91 and 0.93 (against a nominal 95% PI) for predictions of organic carbon and available water capacity in the Edgeroi region of New South Wales, Australia. Tranter *et al*. (2010) examined the relationship between PICP and nominal confidence level between 5% and 95% confidence and noted that PICP began to deviate from the nominal confidence above ~50% confidence.

Odgers *et al*. (2014*b*) suggested that the PROPR algorithm may be particularly useful in situations where site data are limiting and that the knowledge of experts may be the most readily available source of data. This is true, even if we merely get a good picture of the regional trend at the expense of precise local predictions. Of course, in some areas—such as remote lands not suitable for human use—this may be entirely adequate, especially if estimates of uncertainty are available to accompany the regional trend.

Finally, this exercise is valuable because it shows where our soil knowledge in WA and SA needs to be supplemented: the distribution of heavy-textured soils and measurements at depth in the soil profile, in high-clay soils (and very low-clay soils in SA), and generally across most of the centre and north of WA. Algorithms are available (e.g. Carré *et al.* 2007) that allow statistically optimal sampling designs to be identified for filling in the gaps. The underestimation of uncertainty in several of the generalised texture grades superficially suggests that soils are more variable than we have assumed. In addition, this work demonstrates the harmonisation that can be achieved by producing digital soil maps to a common specification without first harmonising the underlying data (e.g. soil classification system) from different jurisdictions.

## Practical considerations

The practicality of wide PI limits is an issue that may deserve debate (Helmick *et al.* 2014). Khosravi *et al*. (2011) argued that PIs too wide are effectively useless and suggested that normalising the PI range against an acceptable target range may aid comparability; this may be an avenue for further research.

In order to employ PROPR over very large areas, the steps required to derive the triangular parameters for each soil class are likely to be case-specific. For example, although Odgers *et al*. (2015) were able to estimate the triangular distributions that represented the within-soil-class variability of pH from observed profiles, expert knowledge played a more prominent role in our case. It is not clear whether we should expect better results by using input data of one kind or another, because it appears that the performance of PROPR's output is also highly dependent on the quality of the probability rasters. Practical implementation of PROPR is complicated by the fact that representativeness of both legacy observations and expert knowledge may be incomplete for a given study area. Often, hard data are not available or are sparse, or have not been sampled with statistical consideration in mind (Minasny *et al*. 2008).

Another practical issue is whether to stratify the study area in order to carry out the spatial prediction. The user may decide that this is necessary because the study area is too large to process in one session or because there is evidence that it would optimise the prediction domain (such as if there were large environmental gradients across the study area). In WA, this was done at the spatial disaggregation stage largely because of processing considerations (Holmes *et al*. 2015).

It could also be beneficial to stratify the spatial domain of the triangular parameter estimates into areas where soil–landscape relations are relatively consistent. When we ran PROPR, we did this in WA by physiographic zone because the properties for the soil classes varied between them. Catchment basins are probably the most intuitive strata because they are delineated relatively easily and because they are usually the products of a relatively consistent set of geomorphic processes (Lotspeich 1980).

## Conclusions

The PROPR algorithm produced a set of digital soil property maps that are a plausible depiction of the spatial pattern of clay content in WA and the agricultural region of SA. The prediction of clay content at each depth interval is modestly supported by the site data in both WA and SA. The predicted clay content of sandy-site data was overestimated and that of clayey-site data was underestimated. The degree of overestimation worsens with depth for sands and improves with depth for clays; thus, the best predicted soils are sands on the surface and clays at depth. This reflects the texture grades commonly observed in the study areas at these depths. Partitioning the validation into areas with different soil characteristics reveals better performance than the global validation.

The maps of clay for WA and SA were produced according to a common specification even though the information on which they are based was derived from legacy maps produced over a long period, at different spatial scales and according to different specifications.

## Acknowledgements

This work was funded by the Australian Government's Terrestrial Ecology Research Network (TERN) Soil and Landscape Grid of Australia Facility. The authors gratefully acknowledge the provision of the soil data for this work from the Department of Agriculture and Food Western Australia and the Department of Environment, Water and Natural Resources (South Australia).

## References

Arnold RW (1966) Differentiation of soils having cyclic or recurring horizons. *Canadian Journal of Soil Science* **46**, 69–74. doi:10.4141/cjss66-010

Bishop TFA, Daniel R, Guest DI, Nelson MA, Chang C (2012) A digital soil map of *Phytophthora cinnamomi* in the Gondwana Rainforests of eastern Australia. In 'Digital Soil Assessments and Beyond: Proceedings of the Fifth Global Workshop on Digital Soil Mapping'. Sydney, NSW, 10–13 April 2012. (Eds B Minasny, BP Malone, AB McBratney) pp. 65–68. (Taylor & Francis: London)

Bui EN, Moran CJ (2001) Disaggregation of polygons of surficial geology and soil maps using spatial modelling and legacy data. *Geoderma* **103**, 79–94. doi:10.1016/S0016-7061(01)00070-2

Carré F, McBratney AB, Minasny B (2007) Estimation and potential improvement of the quality of legacy soil samples for digital soil mapping. *Geoderma* **141**, 1–14. doi:10.1016/j.geoderma.2007.01.018

Clifford D, Guo Y (2015) Methods to merge disparate spatial estimates of soil attributes. *Soil Research* **53**, in press.

De Benedetto D, Castrignanò A, Sollitto D, Modugno F, Buttafuoco G, Io Papa G (2012) Integrating geophysical and geostatistical techniques to map the spatial variation of clay. *Geoderma* **171–172**, 53–63. doi:10.1016/j.geoderma.2011.05.005

DEWNR (2014*a*) SA-format soil and land attributes. Department of Environment, Water and Natural Resources, Adelaide, S. Aust. Available at: www.environment.sa.gov.au/Science/Information_data/soil-and-land/describing-soil-land/sa-format (accessed 1 August 2014).

DEWNR (2014*b*) National-format soil and land attributes. Department of Environment, Water and Natural Resources, Adelaide, S. Aust. Available at: www.environment.sa.gov.au/Knowledge_Bank/Information_data/soil-and-land/describing-soil-land/national-format (accessed 4 August 2014).

FAO (2014) World Reference Base For Soil Resources. World Soil Resources Reports No. 106. (Food and Agriculture Organisation of the United Nations: Rome)

Galbraith JM, Kleinman PJA, Bryant RB (2003) Sources of uncertainty affecting soil organic carbon estimates in northern New York. *Soil Science Society of America Journal* **67**, 1206–1212. doi:10.2136/sssaj2003.1206

Gallichand J, Marcotte D (1993) Mapping clay content for subsurface drainage in the Nile Delta. *Geoderma* **58**, 165–179. doi:10.1016/0016-7061(93)90040-R

Gibbons FR (1983) Soil mapping in Australia. In 'Soils: an Australian viewpoint'. pp. 267–276. (CSIRO/Academic Press: Melbourne/London)

GlobalSoilMap Science Committee (2013) Specifications: Tiered GlobalSoilMap.net Products, Release 2.3. http://globalsoilmap.net/specifications

Gomez C, Lagacherie P, Bacha S (2012) Using Vis-NIR hyperspectral data to map topsoil properties over bare soils in the Cap Bon region, Tunisia. In 'Digital soil assessments and beyond: Proceedings of the Fifth Global Workshop on Digital Soil Mapping'. 10–13 April 2012, Sydney, NSW. (Eds B Minasny, BP Malone, AB McBratney) pp. 387–392. (Taylor & Francis: London)

Grundy MJ, Viscarra Rossel RA, Searle R (2015) The Australian Soil and Landscape Grid: features, derivation and context. *Soil Research* **53**, in press.

Hall JAS, Maschmedt DJ, Billing NB (2009) 'The soils of southern South Australia. Geological Survey of South Australia.' The South Australian Land and Soil Book Series No. 1. (Government of South Australia: Adelaide)

Häring T, Dietz E, Osenstetter S, Koschitzki T, Schröder B (2012) Spatial disaggregation of complex soil map units: A decision-tree based approach in Bavarian forest soils. *Geoderma* **185–186**, 37–47. doi:10.1016/j.geoderma.2012.04.001

Helmick JL, Nauman TW, Thompson JA (2014) Developing and assessing prediction intervals for soil property maps derived from legacy databases. In 'GlobalSoilMap: Basis of the global spatial soil information system'. (Eds D Arrouays, NJ McKenzie, JW Hempel, AC Richer de Forges, AB McBratney) pp. 359–366. (Taylor & Francis: London)

Henderson BL, Bui EN, Moran CJ, Simon DAP (2005) Australia-wide predictions of soil properties using decision trees. *Geoderma* **124**, 383–398. doi:10.1016/j.geoderma.2004.06.007

Holmes KW, Odgers NP, Griffin EA, van Gool D (2014) Spatial disaggregation of conventional soil mapping across Western Australia using DSMART. In 'GlobalSoilMap: Basis of the global spatial soil information system'. (Eds D Arrouays, NJ McKenzie, JW Hempel, AC Richer de Forges, AB McBratney) pp. 273–279. (Taylor & Francis: London)

Holmes KW, Griffin EA, Odgers NP (2015) Continental scale spatial disaggregation of legacy soil maps: evaluation over Western Australia. *Soil Research* **53**, in press.

Hong SY, Kim YH, Han KH, Hyun BK, Zhang YS, Song KC, Minasny B, McBratney AB (2012). Digital soil mapping of soil properties for Korean soils. In 'Digital Soil Assessments and Beyond: Proceedings of the Fifth Global Workshop on Digital Soil Mapping'. Sydney, Australia, 10–13 April 2012. (Eds B Minasny, BP Malone, AB McBratney) pp. 435–438. (Taylor & Francis: London)

Huang J, Wong VNL, Triantafilis J (2014) Mapping soil salinity and pH across an estuarine and alluvial plain using electromagnetic and digital elevation model data. *Soil Use and Management* **30**, 394–402. doi:10.1111/sum.12122

Isbell RF (1996) 'The Australian Soil Classification.' (CSIRO Publishing: Melbourne)

Khosravi A, Mazloumi E, Nahavandi S, Creighton D, van Lint JWC (2011) A genetic algorithm-based method for improving quality of travel time prediction intervals. *Transportation Research Part C, Emerging Technologies* **19**, 1364–1376. doi:10.1016/j.trc.2011.04.002

Kidd DB, Malone BP, McBratney AB, Minasny B, Webb MA (2014) Digital mapping of a soil drainage index for irrigated enterprise suitability in Tasmania, Australia. *Soil Research* **52**, 107–119. doi:10.1071/SR13100

Kotz S, van Dorp JR (2004) 'Beyond beta: other continuous families of distributions with bounded support and applications.' (World Scientific: Singapore)

Lamsal S, Mishra U (2010) Mapping soil textural fractions across a large watershed in north-east Florida. *Journal of Environmental Management* **91**, 1686–1694. doi:10.1016/j.jenvman.2010.03.015

Lawes RA, Oliver YM, Robertson MJ (2009) Integrating the effects of climate and plant available soil water holding capacity on wheat yield. *Field Crops Research* **113**, 297–305. doi:10.1016/j.fcr.2009.06.008

Lin LI-K (1989) A concordance correlation coefficient to evaluate reproducibility. *Biometrics* **45**, 255–268. doi:10.2307/2532051

Lotspeich FB (1980) Watersheds as the basic ecosystem: this conceptual framework provides a basis for a natural classification system. *Journal of the American Water Resources Association* **16**, 581–586. doi:10.1111/j.1752-1688.1980.tb02434.x

Malone BP, McBratney AB, Minasny B, Laslett GM (2009) Mapping continuous depth functions of soil carbon storage and available water capacity. *Geoderma* **154**, 138–152. doi:10.1016/j.geoderma.2009.10.007

Malone BP, McBratney AB, Minasny B (2011) Empirical estimates of uncertainty for mapping continuous depth functions of soil attributes. *Geoderma* **160**, 614–626. doi:10.1016/j.geoderma.2010.11.013

McDonald RC, Isbell RF (2009) Soil profile. In 'Australian soil and land survey field handbook'. 3rd edn. pp. 147–204. (CSIRO Publishing: Melbourne)

McKenzie NJ, Jacquier D, Maschmedt DJ, Griffin EA, Brough DM (2012) 'The Australian Soil Resource Information System (ASRIS) technical specifications (Revised Version 1.6, June 2012).' Australian Collaborative Land Evaluation Program, Canberra, ACT. (CSIRO, Department of Agriculture: Canberra, ACT)

Minasny B, McBratney AB, Lark RM (2008) Digital soil mapping technologies for countries with sparse data infrastructures. In 'Digital soil mapping with limited data'. (Eds AE Hartemink, AB McBratney, M de L Mendonça Santos) pp. 15–30. (Springer: Berlin, Heidelberg)

Nauman TW, Thompson JA (2014) Semi-automated disaggregation of conventional soil maps using knowledge driven data mining and classification trees. *Geoderma* **213**, 385–399. doi:10.1016/j.geoderma.2013.08.024

Odeh IOA, Crawford M, McBratney AB (2006) Digital mapping of soil attributes for regional and catchment modelling, using ancillary covariates, statistical and geostatistical techniques. In 'Digital soil mapping: an introductory perspective'. Developments in Soil Science 31. (Eds P Lagacherie, AB McBratney, M Voltz) pp. 437–453. (Elsevier: Amsterdam)

Odgers NP, Libohova Z, Thompson JA (2012) Equal-area spline functions applied to a legacy soil database to create weighted-means maps of soil organic carbon at a continental scale. *Geoderma* **189–190**, 153–163. doi:10.1016/j.geoderma.2012.05.026

Odgers NP, McBratney AB, Minasny B (2014*a*) Digital soil property mapping and uncertainty estimation using soil class probability rasters. In 'GlobalSoilMap: basis of the global spatial soil information system'. (Eds D Arrouays, NJ McKenzie, JW Hempel, A Richer de Forges, AB McBratney) pp. 341–346. (Taylor & Francis: London)

Odgers NP, Sun W, McBratney AB, Minasny B, Clifford D (2014*b*) Disaggregating and harmonising soil map units through resampled classification trees. *Geoderma* **214–215**, 91–100. doi:10.1016/j.geoderma.2013.09.024

Odgers NP, McBratney AB, Minasny B (2015) Digital soil property mapping and uncertainty estimation using soil class probability rasters. *Geoderma* **237–238**, 190–198. doi:10.1016/j.geoderma.2014.09.009

Pásztor L, Szabó J, Bakacsi Z (2010) Digital processing and upgrading of legacy data collected during the 1 : 25,000 scale Kreybig soil survey. *Acta Geodaetica et Geophysica Hungarica* **45**, 127–136. doi:10.1556/AGeod.45.2010.1.18

Protz R, Presant EW, Arnold RW (1968) Establishment of the modal profile and measurement of variability within a soil landform unit. *Canadian Journal of Soil Science* **48**, 7–19. doi:10.4141/cjss68-002

Schoknecht N, Pathan S (2013) Soil groups of Western Australia. Resource Management Technical Report No. 380. Department of Agriculture and Food Western Australia, South Perth, W. Aust.

Schoknecht N, Tille P, Purdie B (2004) Soil-landscape mapping in south-western Australia. Resource Management Technical Report No. 280. Department of Agriculture and Food Western Australia, South Perth, W. Aust.

Shrestha DL, Solomatine DP (2006) Machine learning approaches for estimation of prediction interval for the model output. *Neural Networks* **19**, 225–235. doi:10.1016/j.neunet.2006.01.012

Soil Survey Staff (1999) 'Soil taxonomy: a basic system of soil classification for making and interpreting soil surveys.' 2nd edn (United States Department of Agriculture Natural Resources Conservation Service: Washington, DC)

Soil Survey Staff (2006) 'U.S. General Soil Map (STATSGO2).' (Natural Resources Conservation Service, United States Department of Agriculture: Washington, DC).

Subburayalu S, Jenhani I, Slater BK (2014) Disaggregation of component soil series using possibilistic decision trees from an Ohio County soil survey map. *Geoderma* **213**, 334–345. doi:10.1016/j.geoderma.2013.08.018

Sun W, McBratney AB, Hempel JW, Minasny B, Malone BP, D'Avello T, Burras L, Thompson JA (2010) Digital harmonisation of adjacent analogue soil survey areas—4. Iowa counties. In 'Proceedings of the 4th Global Workshop on Digital Soil Mapping'. Rome. (International Society of Soil Sciences)

Taylor JK (1970) The development of soil survey and field pedology in Australia, 1927–67. (CSIRO: Melbourne)

Thompson JA, Prescott T, Moore AC, Bell J, Kautz DR, Hempel JW, Waltman SW, Perry CH (2010) Regional approach to soil property mapping using legacy data and spatial disaggregation techniques. In '19th World Congress of Soil Science'. Brisbane, Queensland. (International Society of Soil Sciences)

Tranter G, Minasny B, McBratney AB (2010) Estimating pedotransfer function prediction limits using fuzzy *k*-means with extragrades. *Soil Science Society of America Journal* **74**, 1967–1975. doi:10.2136/sssaj2009.0106

Triantafilis J, Lesch SM (2005) Mapping clay content variation using electromagnetic induction techniques. *Computers and Electronics in Agriculture* **46**, 203–237. doi:10.1016/j.compag.2004.11.006

Triantafilis J, Huckel AI, Odeh IOA (2001) Comparison of statistical prediction methods for estimating field-scale clay content using different combinations of ancillary variables. *Soil Science* **166**, 415–427. doi:10.1097/00010694-200106000-00007

Viscarra Rossel RA, Chen C, Grundy MJ, Searle R, Clifford D, Campbell PH (2015) The Australian three-dimensional soil grid: Australia's contribution to the GlobalSoilMap project. *Soil Research* **53**, in press.

Zhao Z, Chow TL, Rees HW, Yang Q, Xing Z, Meng F-R (2009) Predict soil texture distributions using an artificial neural network model. *Computers and Electronics in Agriculture* **65**, 36–48. doi:10.1016/j.compag.2008.07.008

Zhu AX, Band LE (1994) A knowledge-based approach to data integration for soil mapping. *Canadian Journal of Remote Sensing* **20**, 408–418. doi:10.1080/07038992.1994.10874583

Zhu AX, Band LE, Vertessy R, Dutton B (1997) Derivation of soil properties using a Soil Land Inference Model (SoLIM). *Soil Science Society of America Journal* **61**, 523–533. doi:10.2136/sssaj1997.03615995006100020022x

Zhu AX, Hudson B, Burt JE, Lubich K, Simonson D (2001) Soil mapping using GIS, expert knowledge, and fuzzy logic. *Soil Science Society of America Journal* **65**, 1463–1472. doi:10.2136/sssaj2001.6551463x